Virology 533 (2019) 68–76

Contents lists available at ScienceDirect

Virology

journal homepage: www.elsevier.com/locate/virology

NSP2 forms viroplasms during Dendrolimus punctatus cypovirus infection

Congrui Xu[a,b], Jia Wang[a,b], Jian Yang[a,b], Chengfeng Lei[a], Jia Hu[a], Xiulian Sun[a,*]

[a] Wuhan Institute of Virology, Chinese Academy of Sciences, Wuhan, 430071, Hubei, China
[b] University of Chinese Academy of Sciences, Beijing, 100049, China

ARTICLE INFO

Keywords:
Cypovirus
Viroplasm
NSP2

ABSTRACT

Reoviruses are thought to replicate and assemble in special cytoplasmic structures called 'viroplasms'. However, little is known about the viroplasms of the insect reoviruses, the cypoviruses. To investigate the viroplasm of Dendrolimus punctatus cypovirus (DpCPV), all proteins encoded by the 10 genomic segments of DpCPV were expressed in Sf9 cells using the Bac-to-Bac system. The viral nonstructural protein NSP2 formed viroplasm-like dots which showed close apposition with the endoplasmic reticulum and were surrounded by intracellular membranes during transfection. Colocalization and coimmunoprecipitation assays showed that NSP2 interacts with 4 of 6 structural proteins and another 2 nonstructural proteins, while NSP1 only colocalized with VP4, and NSP3 did not colocalize with any structural protein. Immunoelectron microscopy revealed that NSP2 were nearby the endoplasmic reticulum and mitochondria, and viral particles were present in the electron-dense inclusions formed by NSP2. We proposed that NSP2 is responsible for forming the viroplasms structures of DpCPV.

1. Introduction

The specific intracellular structures that occur during the replication and assembly of many viruses are called viroplasms (Fabbretti et al., 1999; Mohan et al., 2003), virus factories (Broering et al., 2002, 2005; Novoa et al., 2005; Wileman, 2007), or viral inclusion bodies (Brookes et al., 1993; Thomas et al., 1990). In the process of viral infection of host cells, viroplasms concentrate the viral proteins, viral genomes, and host-associated cytokines required for viral replication and assembly. Viroplasms are also involved in the release of progeny viral particles (Eaton et al., 1987; Jia et al., 2012; Mao et al., 2013; McNulty et al., 1976; Sharpe et al., 1982; Shimizu et al., 2009; Wei, 2006; Yan et al., 2015). Therefore, understanding the composition and structure of viroplasms should extend our understanding of the replication process of viruses.

The members of the family *Reoviridae* are RNA viruses whose genomes consist of multiple double-stranded RNA (dsRNA) segments (Roy, 2006). Viroplasms have been detected in the orthoreoviruses (Becker et al., 2003; Broering et al., 2002, 2005), *Fijivirus* (Jia et al., 2012; Mao et al., 2013), and *Aquareovirus* (Ke et al., 2013; Yan et al., 2015). The key viral proteins associated with the formation of viroplasms are nonstructural proteins, e.g., μNS of the reoviruses, nonstructural protein P9-1 of Southern rice black-streaked dwarf virus, and NS80 of Grass carp reovirus (Jia et al., 2012; Ke et al., 2013). Viroplasms are the sites of viral assembly, the nonstructural proteins which take charge to form viroplasms also recruit structural proteins, and other nonstructural proteins into the inclusion bodies, so they interact or colocalize with most of the viral proteins (Broering et al., 2002; Jia et al., 2012; Ke et al., 2013).

The insect reovirus, *Cypovirus* (CPV), is the only known reovirus that forms polyhedra, which only appear in the cytoplasm of insect midgut epithelial cells (Mori and Metcalf, 2010). The polyhedral structure of CPV plays an important role in protecting virion activity (Belloncik, 1989). When the polyhedra are ingested in the midgut of the host, the virions are released and mediate virion-specific infection of intestinal epithelial cells in the host (Chiu et al., 2012). The virions of CPV have a single-layer capsid structure, and they appear as regular icosahedrons with A-spikes, which are not found in other reoviruses (Cheng et al., 2011; Nibert and Baker, 2003; Yu et al., 2011). DpCPV is an important pathogen of *Dendrolimus punctatus* (Kunimi, 2007), which is considered the most destructive pest of pine forests worldwide. Its genome consists of 10 segments of dsRNA, in which the S5, S8, S9, and S10 genes encode the nonstructural proteins NSP1, NSP2, NSP3, and Polyhedrin (Polh), respectively. The remaining genomic segments encode six structural proteins (VP1, RdRp, VP2, VP3, VP4, and VP5) (Chakrabarti et al., 2010; Echeverry et al., 1997; Hagiwara and Matsumoto, 2000; Hagiwara et al., 2002; Rao et al., 2003; Yang et al., 2013).

The functions of the cypovirus nonstructural proteins are poorly

* Corresponding author.
E-mail address: sunxl@wh.iov.cn (X. Sun).

https://doi.org/10.1016/j.virol.2019.05.005
Received 18 March 2019; Received in revised form 14 May 2019; Accepted 15 May 2019
Available online 16 May 2019
0042-6822/

elaborated. In this study, we used a baculovirus expression system (Airenne et al., 2000) to express all the proteins encoded by the DpCPV genomic segments in Sf9 cells to study their relationships with viroplasms. Based on the subcellular localization of NSP2 and its interactions with other viral proteins or host cell organelles, together with an immunoelectron microscopic analysis using an *anti*-NSP2 antibody, we conclude that NSP2 forms the viroplasms during DpCPV infection.

2. Materials and methods

2.1. Cell lines, viruses, and antibodies

DpCPV was originally isolated from the larvae of *D. punctatus* and propagated in *Spodoptera exigua* larvae (Cheng et al., 2014). *Escherichia coli* DH5α (Invitrogen, Carlsbad, CA, USA), the pFastBac™ Dual donor plasmid (Invitrogen), and *E. coli* DH10B (Invitrogen) containing an AcBacmid and a helper plasmid were used for the construction of the recombinant baculoviruses expressing DpCPV proteins. The Sf9 cell line (Invitrogen) was used for the transfection and infection of the recombinant baculoviruses. The cells were cultured at 27 °C in Grace medium containing 10% (v/v) fetal bovine serum (FBS; Thermo Fisher Scientific, Waltham, MA, USA). A laboratory colony of *S. exigua* larvae were reared at 27 °C on an artificial diet. The antibodies used in the experiments included an *anti*-mCherry polyclonal antibody (pAb), *anti*-GFP pAb, anti-Flag pAb, and *anti*-PDI pAb (Proteintech, Wuhan, China). The *anti*-NSP2 pAb was prepared by inoculating rabbits with NSP2 expressed in *E. coli*.

2.2. DpCPV infection of Sf9 cells

CPV virions embedded in the polyhedral structure which only degrades under alkaline conditions. In order to promote virus infection of cells, a suspension of purified DpCPV polyhedra, with a density of 1.52×10^8/mL, was cleaved with 0.2 mol/L Na_2CO_3–$NaHCO_3$ (pH 10.8) to clarification at room temperature. The pH was adjusted to 7.4 with 1 mol/L Tris-HCl (pH 6.8) buffer and centrifuged at 4000 × *g* for 5 min. The supernatant was collected, mixed with serum-free Grace medium, filter-sterilized, and added to Sf9 cells placed in glass vials. After incubation for 6 h, the cells were replaced with Grace medium containing 10% (v/v) FBS, and the cells were harvested 5 days after infection.

2.3. Collection of recombinant baculoviruses expressing DpCPV proteins

DNA fragments encoding each gene of DpCPV were amplified with reverse transcription PCR (Cheng et al., 2014). The marker-fused coding sequences of each viral protein gene was then purified and cloned into the pFastBac™ Dual vector (Invitrogen) by FastCloning (Li et al., 2011), using the primers listed in Table 1. Briefly, the vector and insert were amplified with PCR, wherein the insert had a vector 16 bp homologous sequence. The DNA templates were digested with *Dpn*I, and the digestion products were used to transform competent cells. The *eGFP* and *mCherry* DNA fragments were amplified from pIB/V5$^{EGFP–Rab5}$ and pIZ/V5$^{mCherry–Rab7}$, respectively (Qin et al., 2019). The sequences encoding structural proteins, fused with *eGFP* at the 3′-end, and those encoding nonstructural proteins, fused with *mCherry* at the 5′-end, were inserted under the control of the *p10* and *polyhedrin* promoters (P_{P10} and P_{PH}), respectively (Fig. 1A). Competent *E. coli* DH10Bac cells were then transformed with the resulting pFastBac™ Dual vectors to express the DpCPV proteins.

Sf9 cells were transfected with these bacmids using Cellfectin® Reagent (Invitrogen), according to the manufacturer's instructions. Briefly, Sf9 cells were plated in glass-bottomed culture dishes at a cell density of 8×10^5 cells, the 200 µl of Grace' insect medium containing 8 µl of Cellfectin Reagent and 3 µg of bacmid was added. The cells were incubated at 27 °C for 5 h and the medium was then replaced with Grace insect medium containing 10% FBS. After incubation at 27 °C for 72 h, the supernatant was collected and centrifuged at 500 × *g* for 5 min to remove the cells and large debris. The supernatant was transferred to a new sterile centrifuge tube. The P1 generation of budded recombinant viruses was stored at 4 °C in the dark.

2.4. Construction of DpCPV NSPs stable cell line

The *mCherry-nsp2*, *mCherry-nsp3* fusion sequences were ligated into the multiple cloning site region of the plasmid vector pIB/V5-His. Sf9 cells were separatedly transfected with the constructed plasmid vectors expressing the DpCPV non-structural proteins NSP2, NSP3, and a dish of cells not transfected with the plasmid was used as a control. At 48 h post transfection (h.p.t.), blasticidin (Thermo Fisher Scientific) with a final concentration of 60 µg/m was added to the medium of each group of cells to perform screening of the cell line. After all the cells in the control group died, about 1 week, a stable expression cell line was obtained. In the subsequent subcultures of the above stable expression cell lines, a final concentration of 30 µg/m of blasticidin was continuously added to the medium to maintain the selection pressure.

2.5. Fluorescence colocalization assays

An aliquot (50 µl) of the budded viruses of each recombinant baculovirus expressing a DpCPV structural protein or a nonstructural protein was collected, mixed well in an Eppendorf tube, added to cultured Sf9 cells in glass-bottomed culture dishes, and incubated at 27 °C for 72 h. The cells were then fixed with 4% paraformaldehyde for 10 min at room temperature, and washed three times with phosphate-buffered saline (PBS) for 3 min each. A final concentration of 1 µg/ml Hoechst solution was added to stain the cells for 5 min at room temperature. The cells were washed three times with PBS for 3 min each. The colocalization of the structural and nonstructural proteins in the treated cells was observed with a 60 × oil-immersion objective with the PerkinElmer UltraView VOX system. The nuclear Hoechst dye, eGFP tag, and mCherry tag were excited at 405 nm, 488 nm, and 561 nm, respectively. An image analysis of the experimental results was performed with the ImageJ software (https://imagej.nih.gov/ij/).

2.6. Immunofluorescent labeling of endoplasmic reticulum (ER) and intracellular membrane

Sf9 cells cultured in glass-bottomed culture dishes were infected with the recombinant viruses and incubated at 27 °C for 72 h. The cells were fixed with 4% paraformaldehyde for 10 min at room temperature and permeabilized with 0.2% Triton X-100 for 10 min at room temperature. The cells were washed three times with PBS for 3 min each. A blocking solution of bovine serum albumin (5%) containing 0.1% Tween 20 (PBST–BSA) was added and the cells incubated for 30 min at 37 °C. The primary antibody diluted with PBST–BSA was added, and the cells were incubated at 37 °C for 1 h and washed three times with PBS for 3 min each. The DpCPV viral protein was probed with an anti-Flag antibody (Proteintech) and the ER was probed with an anti-protein disulfide isomerase (PDI) antibody (Proteintech) (Goo et al., 2003). A PBST–BSA-diluted secondary antibody (Alexa-Fluor-labeled goat anti-rabbit or goat anti-mouse IgG antibody) was added, and the cells were incubated at 37 °C for 1 h and washed three times for 3 min each. The cell nuclei were labeled with Hoechst solution at a final concentration of 1 µg/ml. The intracellular membrane was labeled with the fluorescent dye 3,3′-dioctadecyloxacarbocyanine perchlorate (DiO) (Beyotime, Shanghai, China). Specifically, after the cells were infected with the recombinant baculovirus for 6 h, DiO was added to the culture medium at a final concentration of 7.57 µmol/L. The colocalization of the structural and nonstructural proteins in the treated cells was observed with a 60 × oil-immersion objective with the PerkinElmer UltraView VOX system. The nuclear Hoechst dye, ER, and Flag tag were

Table 1
Primers used in this study.

Primer	Primer Sequence (5′-3′)
vp1-F	ATCACTCGACGAAGACATGCACAGTACTAACAATAATTCAAATAAAC (16 bp vector homologous sequence underlined)
vp1-R	CGCCGCTGCCGCCGCCGGCATTGCGTATATTGATCGCG (16 bp vector homologous sequence underlined)
rdrp-F	ATCACTCGACGAAGACATGTTACCAAACACTGAACTACACA (16 bp vector homologous sequence underlined)
rdrp-R	CGCCGCTGCCGCCGCCCACCGTATCTGCCTCAGGC (16 bp vector homologous sequence underlined)
vp2-F	ATCACTCGACGAAGACATGGAAATAAATAGAGCGGAAATTCG (16 bp vector homologous sequence underlined)
vp2-R	CGCCGCTGCCGCCGCCGAAGAAACCCTTGAAGCGTAATTG (16 bp vector homologous sequence underlined)
vp3-F	ATCACTCGACGAAGACATGTGGCATTATACGAGTATCAAC (16 bp vector homologous sequence underlined)
vp3-R	CGCCGCTGCCGCCGCCCGAGCGTACAAGTTTGATCAC (16 bp vector homologous sequence underlined)
vp4-F	ATCACTCGACGAAGACATGTTCGCAATCGATCCACTC (16 bp vector homologous sequence underlined)
vp4-R	CGCCGCTGCCGCCGCCGTGAACCCACTTCCAACGC (16 bp vector homologous sequence underlined)
vp5-F	ATCACTCGACGAAGACATGTTACAACAACCAGCAGGAG (16 bp vector homologous sequence underlined)
vp5-R	CGCCGCTGCCGCCGCCTAGGATGTCATCTGAGTGCGTA (16 bp vector homologous sequence underlined)
nsp1-F	CCGGAATTCATGGTGAGCAAGGGCGAGGA (SalI Site underlined)
nsp1-R	AAGGAAAAAAGCGGCCGCTTAAATGCCCAGATGTGCCCTG (NotI Site underlined)
nsp2-F	CCGGAATTCATGGTGAGCAAGGGCGAGGA (SalI Site underlined)
nsp2-R	AAGGAAAAAAGCGGCCGCCTACTCTGCCTCTAGAACGC (NotI Site underlined)
nsp3-F	CCGGAATTCATGGTGAGCAAGGGCGAGGA (SalI Site underlined)
nsp3-R	AAGGAAAAAAGCGGCCGCTTACTCTGATACGTCACCATCATC (NotI Site underlined)
polh-F	CCGGAATTCATGGTGAGCAAGGGCGAGGA (SalI Site underlined)
polh-R	AAGGAAAAAAGCGGCCGCTCACTGATGGTTACTCAGAGCTA (NotI Site underlined)

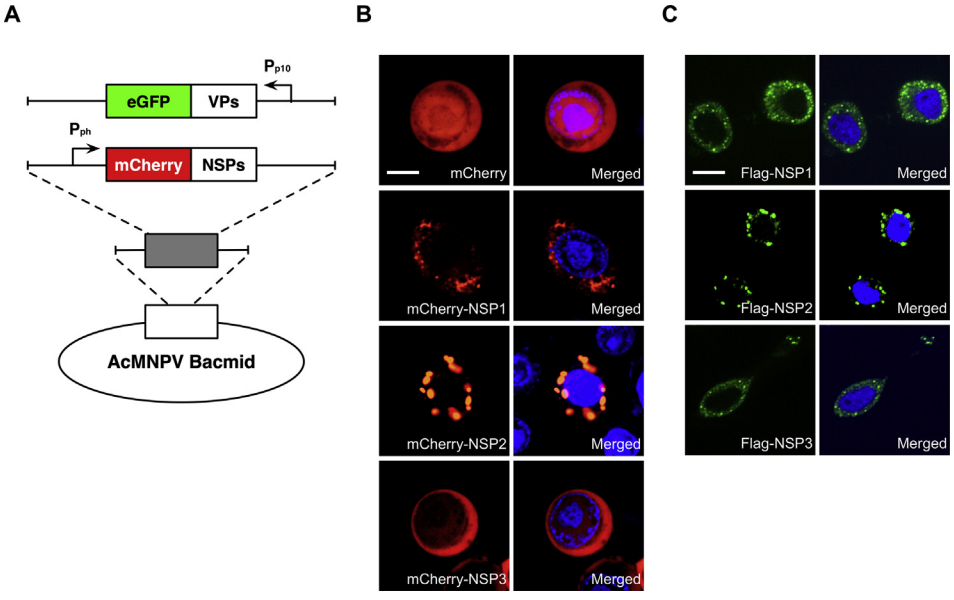

Fig. 1. Construction of recombinant bacmids and localization of DpCPV NSPs in Sf9 cells. (A) Schematic diagram of recombinant baculoviruses expressing DpCPV viral proteins. The nonstructural protein genes of DpCPV were located downstream from the *polyhedron* (PH) promoter (P_{PH}) and fused to the red fluorescent protein gene (*mCherry*) at their 5′ end; the structural protein genes of DpCPV were located downstream from the *p10* promoter (P_{P10}), and the enhanced green fluorescent protein gene (*eGFP*) was fused to their 3′ ends. (B) Localization of DpCPV nonstructural proteins fused to mCherry in Sf9 cells. Sf9 cells were transfected with AcBac-mCherry, AcBac-mCherry–NSP1, AcBac-mCherry–NSP2, or AcBac-mCherry–NSP3. At 3 dpt, the cells were fixed and the nuclei counterstained with Hoechst. Images were recorded. Scale bars, 10 μm. (C) Localization of Flag-tagged DpCPV nonstructural proteins in Sf9 cells. Sf9 cells were transfected with recombinant baculovirus expression vectors encoding Flag-tagged nonstructural proteins, and then fixed 72 h after transfection. Cell nuclei were counterstained with Hoechst. Cells were observed and photographed with a laser confocal microscope. Scale bars, 10 μm.

excited at 405 nm, 488 nm, and 561 nm, respectively. The image analysis of the experimental results was performed with the ImageJ software (https://imagej.nih.gov/ij/).

2.7. Co-immunoprecipitation (co-IP) assays and western blotting (WB) analysis

Dynabeads™ Protein G (50 μl; Thermo Fisher Scientific) were incubated with 10 μg of antibody at 4 °C overnight. Sf9 cells were coinfected with recombinant baculoviruses for 72 h, and collected on ice. After the cells were washed with PBS, 200 μl of cell lysis buffer (Yeasen, Shanghai, China) was added and incubated at 4 °C for 1 h. The cell lysates were added to the antibody-bound Dynabeads and incubated for 2 h at room temperature. The beads were washed three times with PBS containing 1% Tween 20 (PBST), resuspended in 20 μl of 2 × PBS and 5 × sample buffer, and boiled for 10 min. The samples were then loaded onto a 10% SDS-PAGE gel for western blotting analysis. After electrophoresis for 120 min, the proteins were electrotransferred to polyvinylidene difluoride membrane (Millipore, Billerica, MA, USA) for 120 min at 100 V. The membrane was blocked overnight at 4 °C with Tris-buffered saline (TBS) containing 5% nonfat dry milk, and then washed three times with TBS containing 0.1% Tween 20 (TBST) for 15 min each. The membrane was incubated with the indicated primary antibodies (against eGFP or mCherry) at 37 °C for 2 h, and then washed three times with TBST for 15 min each. The membrane was then incubated with the corresponding horseradish-peroxidase-conjugated secondary antibody (Beyotime) for 1.5 h, and washed three times with TBST for 15 min each. The signal was detected with NBT/BCIP reagents (Beyotime).

2.8. Immunoelectron microscopy

Sf9 cells plated in glass-bottomed culture dishes were transfected with the pIB/V5-His plasmid expressing NSP2 or infected with DpCPV.

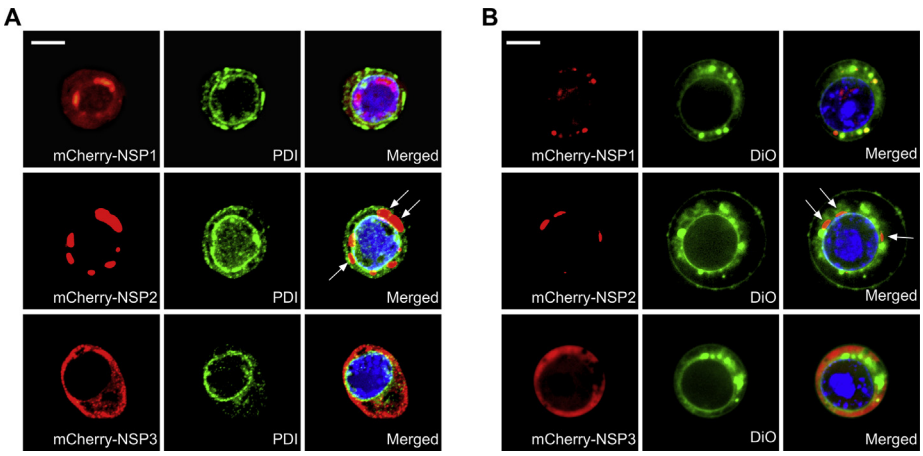

Fig. 2. NSP2 codistributed with the endoplasmic reticulum (ER) and intracellular membrane components. (A) Immunofluorescent colocalization analysis of NSP2 and ER in Sf9 cells. Sf9 cells were infected with recombinant baculoviruses expressing NSPs and polyhedrin (Polh) for 72 h, and immunofluorescence experiments were performed. ER was labeled with *anti*-PDI antibody. Cell nuclei were counterstained with Hoechst. The cells were observed and photographed with laser confocal microscopy. Scale bars, 10 μm. (B) Colocalization of NSP2 and intracellular membrane in Sf9 cells. After cells were infected with a recombinant baculovirus expressing NSPs for 6 h, the intracellular membrane was labeled with DiO, and the cells were fixed at 3 dpi. The cell nuclei were counterstained with Hoechst, and the cells were observed and photographed with a laser confocal microscope. Scale bars, 10 μm.

The cells were collected at 3 days post transfection (d.p.t.) or 5 days post infection (d.p.i.) for immunoelectron microscopic analysis, with a previously described method (Li et al., 2015). Briefly, the cells were fixed with 1% (v/v) paraformaldehyde and 0.5% (v/v) glutaraldehyde in PBS (pH 7.4) for 10 min at 4 °C, and fixed again for 1 h at 4 °C in 2% (v/v) paraformaldehyde and 2.5% (v/v) glutaraldehyde in PBS (pH 7.4). The cells were collected and washed three times with PBS at 4 °C for 10 min each. The cells were fixed and stained with 0.01% citric acid for 30 min and washed three times with PBS at 4 °C for 10 min each. The samples were dehydrated and embedded. Ultrathin sections were cut and immunostained with *anti*-NSP2 pAb (1:50) as the primary antibody. Goat anti-rabbit IgG coated with gold particles (10 nm, Sigma, Darmstadt, Germany) was used as the secondary antibody (1:50). The samples were observed with an FEI Tecnai G^2 20 TWIN transmission electron microscope. Totally 100 viroplasm-like structures were observed and number of those nearby the ER and mitochondria (MI) was quantified.

3. Results

3.1. DpCPV NSP2 forms viroplasm-like aggregations in Sf9 cells

The DpCPV nonstructural proteins NSP1, NSP2, NSP3, and Polh were fused with the fluorescent protein mCherry and expressed in Sf9 cells from bacmids derived from Autographa californica multiple nucleopolyhedrovirus (AcBacmids) (Fig. 1A). At 72 h posttransfection (h.p.t.), a confocal microscopic analysis showed that mCherry-NSP2 formed distinct punctate aggregates, in contrast to the other proteins (Fig. 1B), and that the morphology of these aggregates was similar to those of other reovirus viroplasms (Becker et al., 2003; Broering et al., 2002; Jia et al., 2012; Ke et al., 2013). The mCherry-NSP1 also aggregated in cells, however the size of these aggregates was much smaller that of the reported viroplasm of other reoviruses. There were no nonspecific protein aggregates in cells expressing mCherry-NSP3 or the fluorescent protein (mCherry) alone (Fig. 1B). When the nonstructural proteins of the virus were labeled with the Flag tag, the results of an immunofluorescence assay of the nonstructural proteins of DpCPV alone were similar to those of the fluorescent protein fusion experiments (Fig. 1C), indicating the fluorescent marker proteins did not affect the localization of the viral proteins. These results indicate that the expression of NSP2 alone is sufficient to induce the formation of viroplasm-like structures in Sf9 cells.

3.2. DpCPV NSP2 associates with ER elements in Sf9 cells

Viral viroplasms interact with intracellular membranes in the cytoplasm, including the ER, during the viral infection of host cells (Crawford and Desselberger, 2016; Fernandez de Castro et al., 2014; Romero-Brey and Bartenschlager, 2016). When Sf9 cells were infected with baculoviruses expressing DpCPV NSPs for 72 h and the ER was labeled with an anti- PDI antibody, the green fluorescently labeled ER closely surrounded the dots-like aggregates formed by NSP2. No similar phenomenon was observed when the other viral NSPs were treated in the same way (Fig. 2A). This result is similar to the result for mammalian reovirus viroplasms (Fernandez de Castro et al., 2014), and indicates that there is an association between DpCPV NSP2 and the cellular ER.

We used DiO a cell membrane dye, to stain Sf9 cells infected with individual baculoviruses expressing DpCPV NSPs. The dots formed by NSP2 was located in the intracellular membranes area in the host cells. NSP1 was also located in the intracellular membranes area, but NSP3 does not appear to be clearly associated with intracellular membrane (Fig. 2B). These results indicate that NSP2 is associated with the ER and the intracellular membranes of Sf9 cells.

3.3. NSP2 interacts with most structural proteins of DpCPV

To investigate the relationship between NSP2 and the DpCPV structural proteins, the sequence encoding each structural protein was cloned individually into an AcBacmid for expression fused to enhanced green fluorescent protein (eGFP). After Sf9 cells were separately transfected with the bacmids, VP1, RdRp, and VP3 were ultimately distributed throughout the cytoplasm, whereas VP4 and VP5 agglomerated in the cytoplasm (Fig. 3A). Then we performed the colocalization experiments by using different combinations of recombinant baculoviruses expressing the structural and nonstructural proteins to coinfect Sf9 cells. The results showed that the localization of some structural proteins in cells was altered by expressing of NSP2. The mCherry-NSP2 clearly colocalized with VP1-eGFP, RdRp-eGFP, VP3-eGFP, and VP4-eGFP, but not with VP2-eGFP or VP5-eGFP (Fig. 3B). In contrast, NSP1 only had significant colocalization with VP4, and NSP3 had no significant colocalization with any structural protein (Fig. 4). The results of experiments used stable cell lines expressing NSP2 or NSP3 were consistent with the above results (Fig. 5). The fluorescent proteins did not colocalize with any nonstructural protein (Figs. 3B and 4) and structural protein (Fig. S1).

Co-IP experiments showed that mCherry-NSP2 interacted with VP1-eGFP, RdRp-eGFP, VP3-eGFP, and VP4-eGFP in Sf9 cells (Fig. 3C), consistent with the results of the colocalization analysis.

3.4. NSP2 interacts with the NSPs of DpCPV

In a similar manner, we used fluorescent proteins as markers to study the relationships between NSP2 and the other NSPs of DpCPV.

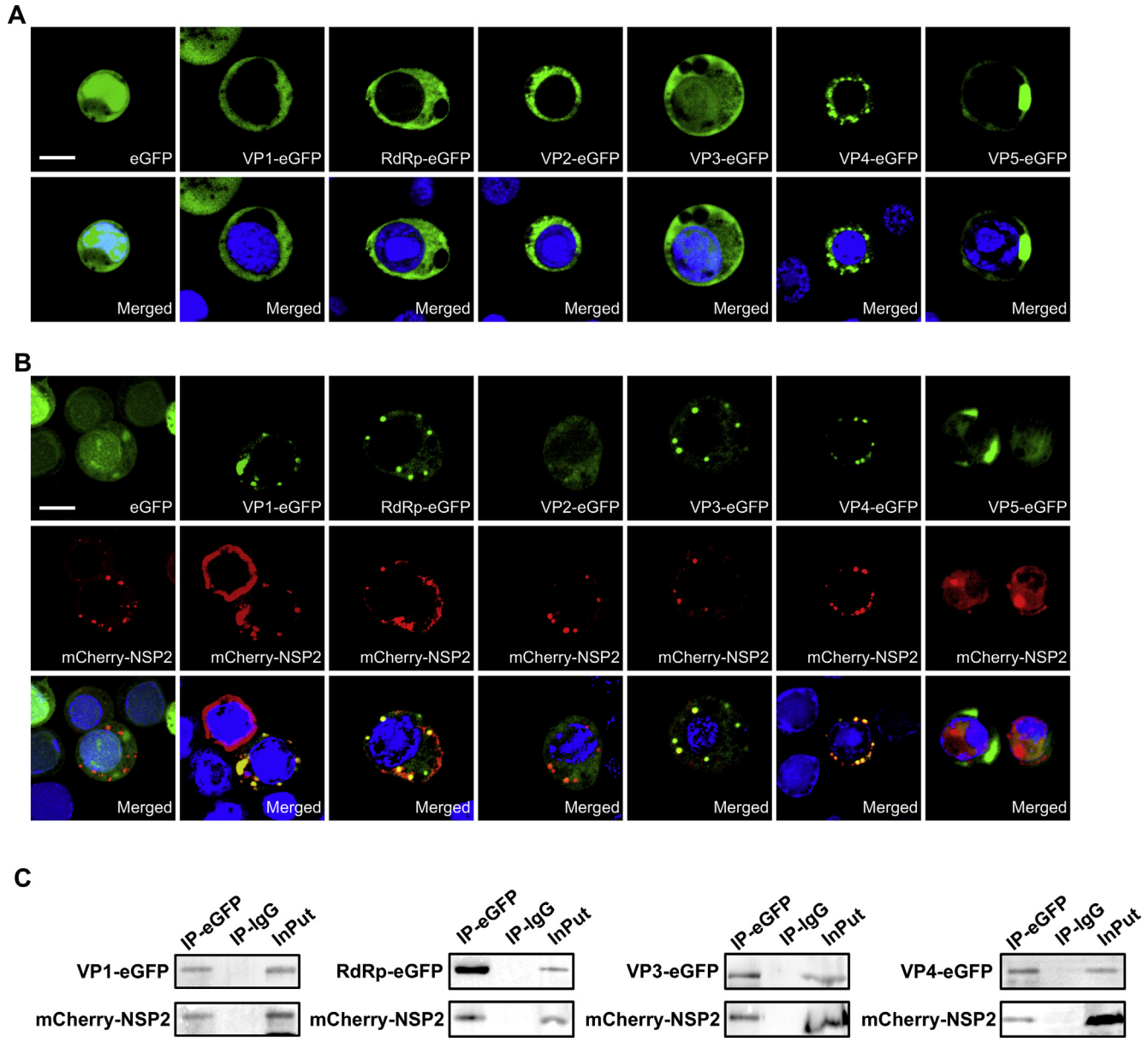

Fig. 3. Interactions of NSP2 with viral structural proteins in Sf9 cells. (A) Localization of DpCPV structural proteins fused to eGFP in Sf9 cells. Sf9 cells were transfected individually with recombinant bacmids expressing viral structural proteins fused to eGFP. At 72 h pt, the cells were fixed, the cell nuclei were counterstained with Hoechst, and the cells were observed and photographed with a laser confocal microscope. Scale bars, 10 μm. (B) Colocalization of DpCPV structural proteins with mCherry-NSP2 in Sf9 cells. Recombinant baculoviruses expressing viral structural proteins and a recombinant baculovirus expressing mCherry-NSP2 were used to coinfect Sf9 cells. The cells were fixed at 72 h.p.i. Cell nuclei were counterstained with Hoechst, and the cells were observed and photographed with a laser confocal microscope. Scale bars, 10 μm. (C) Co-IP assays of structural proteins-eGFP and mCherry-NSP2. Sf9 cells were coinfected with bacmids expressing structural proteins-eGFP and mCherry-NSP2. Cells were lysed and IP assays were performed with polyclonal antibodies against eGFP (IP-VP1, IP-RdRp, IP-VP3, IP-VP4), mCherry (IP-NSP2), or negative control serum (IP-IgG). IP samples were further analyzed with western blotting.

NSP2 was fused to eGFP and the remaining NSPs were labeled with mCherry in a baculovirus expression system. The results showed that NSP2-eGFP clearly colocalized with both mCherry-NSP1 and mCherry-NSP3 (Fig. 6A). Further co-IP assays confirmed these interactions (Fig. 6B).

3.5. Polyhedrin does not colocalize with NSP2 but colocalizes with VP5 in Sf9 cells

Viral polyhedrin labeled with the Flag tag was expressed in Sf9 cells (Fig. 7A) and its interactions with the other proteins of the virus were studied. Colocalization experiments showed that polyhedrin did not colocalize with NSP2-eGFP, whereas it did colocalize with the structural protein VP5-eGFP (Fig. 7B). A co-IP experiment with polyhedrin and VP5 confirmed this interaction (Fig. 7C).

3.6. Viral particles of DpCPV accumulate in inclusions formed by NSP2 in virus-infected Sf9 cells

To confirm that NSP2 forms viroplasms in cells, we used immunogold electron microscopy with an *anti*-NSP2 antibody. Plasmid pIB/V5-His was used as the vector to express NSP2 in Sf9 cells. In the cells expressing NSP2, the gold particles were specifically located in electron-dense inclusions (0.2–0.5 μm), and several inclusions clustered in a large spheroidal structure (1–2 μm) (Fig. 8A). In the samples we observed, 92% of the spheroidal structure located near the ER and

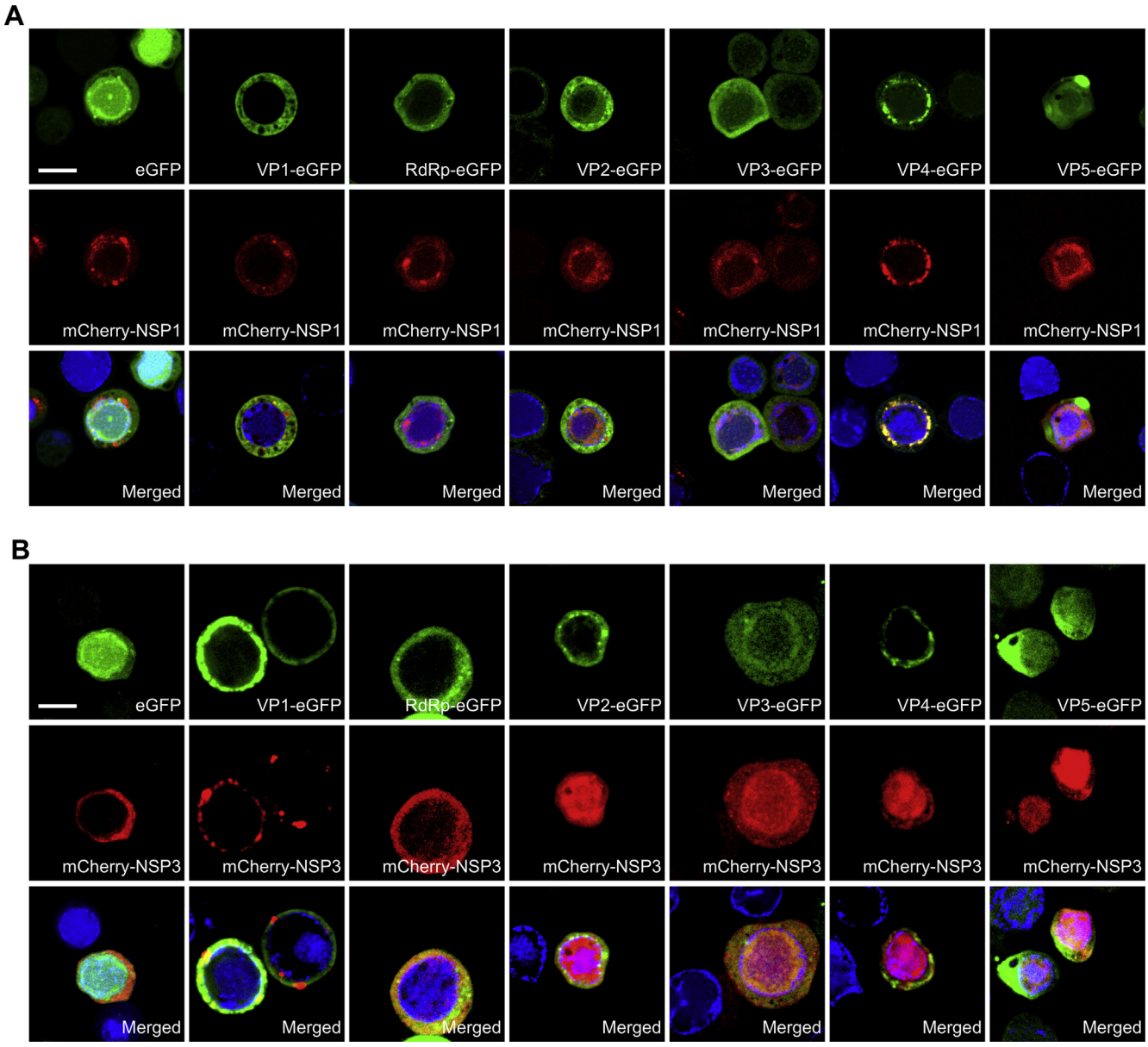

Fig. 4. Colocalization of NSP1 or NSP3 with viral structural proteins in Sf9 cells. (A) Colocalization of DpCPV structural proteins with mCherry-NSP1 in Sf9 cells. Recombinant baculoviruses expressing viral structural proteins and a recombinant baculovirus expressing mCherry-NSP1 were used to coinfect Sf9 cells. The cells were fixed at 72 h.p.i. Cell nuclei were counterstained with Hoechst, and the cells were observed and photographed with a laser confocal microscope. Scale bars, 10 μm. (B) Colocalization of DpCPV structural proteins with mCherry-NSP3 in Sf9 cells. Recombinant baculoviruses expressing viral structural proteins and a recombinant baculovirus expressing mCherry-NSP3 were used to coinfect Sf9 cells. The cells were fixed at 72 h.p.i. Cell nuclei were counterstained with Hoechst, and the cells were observed and photographed with a laser confocal microscope. Scale bars, 10 μm.

mitochondria (MI).

To further clarify the role of NSP2 in viral infection, we used DpCPV virions to infect Sf9 cells and collected the cells at 5 d.p.i. We analyzed them with immunogold electron microscopy using an *anti*-NSP2 antibody. In the cells infected with DpCPV, the gold-particles aggregated on the electron-dense inclusions, which also clustered together in spheroidal structures with similar size of those formed in the cells expressing NSP2 alone, and virions were observed in the electron-dense inclusions (Fig. 8B). These results indicate that NSP2 is an important component of the viroplasms in DpCPV-infected cells.

4. Discussion

To present, many works have focused on the function and formation mechanism of viroplasm for a variety of reoviruses. However, relevant work on CPV can rarely be found. Viroplasm is observed in BmCPV-infected silkworm midgut epithelial cells (Tan et al., 2003), while the mechanism(s) involved in viroplasm formation remains unclear. Studies on other reoviruses suggest that 1–2 non-structural proteins are essential for viroplasm formation (Becker et al., 2003; Fabbretti et al., 1999; Haatveit et al., 2016; Jia et al., 2012; Ke et al., 2013; Wei, 2006). Little is known about the role of viroplasm formation during DpCPV infection. In present study, we screened on non-structural proteins of NSP1, NSP2, NSP3, and Polyhedrin of DpCPV, and found that NSP2 played an essential role in the formation of viroplasm by its interaction with most of structural proteins and nonstructural proteins, and close apposition with intracellular membranes and endoplasmic reticulum.

It has been reported that the rotavirus nonstructural proteins, NSP5 and NSP2, form viroplasm-like structures, and the NSP2 protein binds to the N-terminal region of NSP5 (Fabbretti et al., 1999). Further

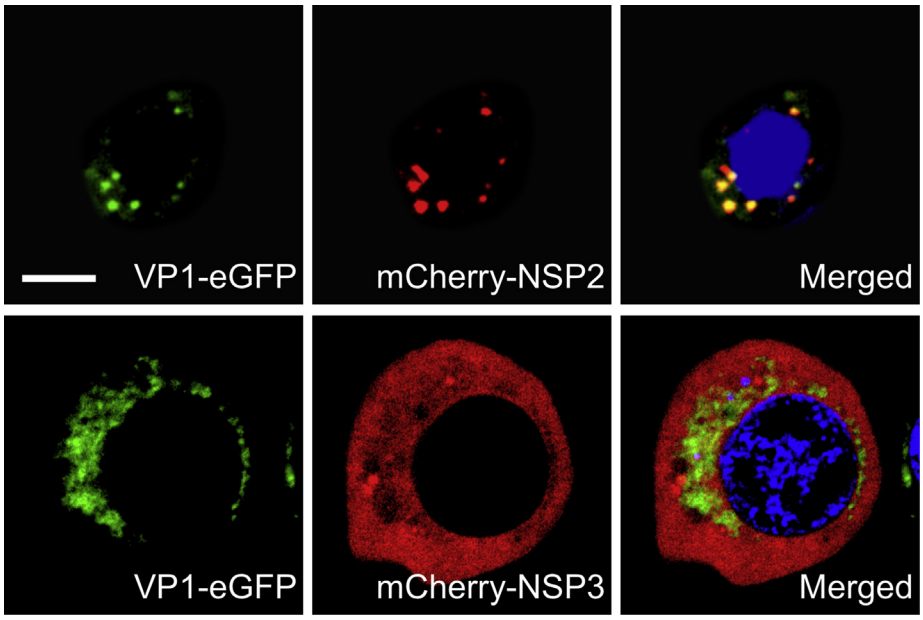

Fig. 5. Colocalization of NSPs with VP1 in cell lines stably expressing NSPs. Sf9 cells were transfected separately with the pIB/V5-His vector expressing individual NSPs. At 48 h.p.t., blasticidin (Thermo Fisher Scientific) at a final concentration of 60 μg/ml was used to select the cell lines. The selection pressure was maintained for 1 month, and cell lines stably expressing the NSPs were obtained. These cell lines were infected with a recombinant baculovirus expressing VP1 and fixed at 72 h.p.i. Cell nuclei were counterstained with Hoechst, and the cells were observed and photographed with a laser confocal microscope. Scale bars, 10 μm.

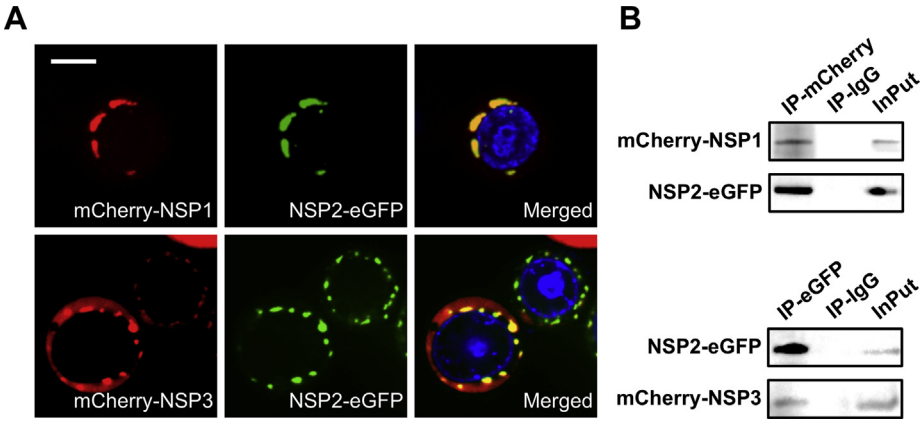

Fig. 6. Interaction of NSP2 with NSP1 or NSP3 in Sf9 cells. (A) Colocalization of DpCPV mCherry-NSP1 or mCherry-NSP3 with NSP2-eGFP in Sf9 cells. Recombinant baculovirus expressing the viral non-structural protein labeled with red fluorescent protein was coinfected with a recombinant baculovirus expressing eGFP-labeled NSP2. The cells were fixed at 72 h.p.i. and the nuclei were counterstained with Hoechst. The cells were observed and photographed with a laser confocal microscope. Scale bars, 10 μm. (B) Co-IP assays of NSPs-mCherry and NSP2-eGFP. Sf9 cells were coinfected with bacmids expressing mCherry-NSP1 or mCherry-NSP3 and NSP2-eGFP. Cells were lysed and IP assays were performed with polyclonal antibodies against mCherry (IP-NSP1, IP-NSP3), eGFP (IP-NSP2), or negative control serum (IP-IgG). IP samples were further analyzed with western blotting.

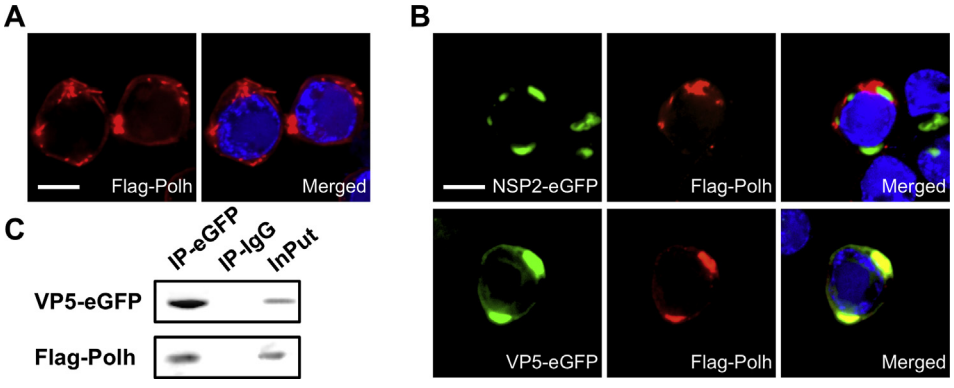

Fig. 7. Colocalization assay of polyhedron (Polh) and NSP2 or VP5 in Sf9 cells. (A) Localization of DpCPV Polh in Sf9 cells. Sf9 cells were infected with a recombinant baculovirus expressing Flag-tagged Polh and fixed at 72 h.p.i. Cell nuclei were counterstained with Hoechst. Cells were observed and photographed with a laser confocal microscope. Scale bars, 10 μm. (B) Colocalization of DpCPV Polh with NSP2-eGFP or VP5-eGFP in Sf9 cells. Cells were coinfected with recombinant baculovirus expressing Flag-tagged Polh and recombinant baculovirus expressing NSP2-eGFP or VP5-eGFP. The cells were fixed at 72 h.p.i. and the nuclei counterstained with Hoechst The cells were observed and photographed with a laser confocal microscope. Scale bars, 10 μm. (C) Co-IP assay of VP5-eGFP and Polh. Sf9 cells were coinfected with bacmids expressing VP5-eGFP or Polh. Cells were lysed and IP assays were performed with polyclonal antibodies against eGFP (IP-VP5), Flag tag (IP-Polh), or negative control serum (IP-IgG). IP samples were further analyzed with western blotting.

studies indicate NSP5 alone is capable of forming viroplasm when its N terminus is blocked, in this case by fusion with either GFP or a hemagglutinin tag, and its C terminus is unmodified (Mohan et al., 2003). In our experiments, whether mCherry was fused at the N-terminus of NSP2 (Fig. 1B), or eGFP was fused at the C-terminus (Fig. 6A), it was able to form a viroplasm-like structure when expressed alone in Sf9 cells. These results indicated that the subcellular localization and aggregation morphology of DpCPV NSP2 in cells were not significantly affected by fusion of the fluorescent proteins.

Further investigations demonstrate that NSP2 protein interacts with viral structural proteins VP1, RdRp, VP3, VP4 and non-structural proteins, NSP1 and NSP3. Among these proteins, VP1 is a capsid

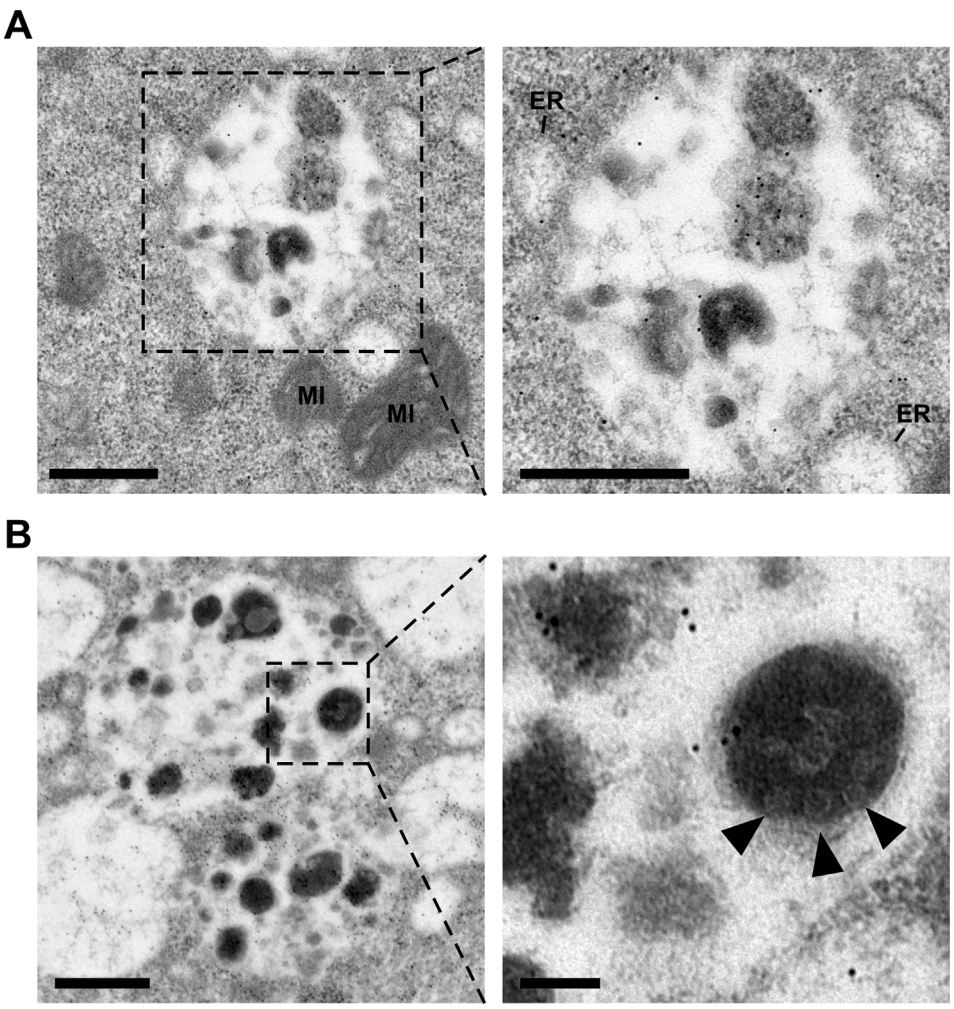

Fig. 8. Immunoelectron microscopic analysis of NSP2 in Sf9 cells. (A) Immunogold labeling of NSP2 expressed in Sf9 cells was associated with electron-dense inclusions. Cells were immunostained with a primary NSP2-specific polyclonal antibody and gold-particle (10 nm diameter)-conjugated goat antibody directed against rabbit IgG as the secondary antibody at 3 dpt. Scale bar, 500 nm. Inset on right showed the viroplasm-like inclusions formed by NSP2 were surrounded by ER. Scale bar, 500 nm. (B) Viral particles were presented in the electron-dense inclusions area associated with immunogold labeling of NSP2 in DpCPV-infected Sf9 cells. Scale bar, 500 nm. Arrows show viral particles in the viroplasm matrix at 5 d.p.i. Scale bar, 100 nm.

component of the DpCPV virion, RdRp is related to the replication of the viral genome, and VP3 is the main component of the pyramidal surface of the virion. By immunoelectron microscopy, NSP2 forms the electron dense inclusions both in NSP2 expressing cells and DpCPV-infected cells, and these inclusions clustered to form a large spheroidal structure. The size of this large structure (1–2 μm) was similar to that of the viroplasm-like structures of other Reoviruses (Jia et al., 2012). This structure might contain other viral proteins and host-associated cytokines required for viral replication and assembly, while NSP2 was the main component as a scaffold.

In addition, NSP1 also co-localizes with the intracellular membrane components, but does not co-localize with the major capsid protein VP1 of DpCPV, indicating that NSP1 might not be the key in formation of viroplasm. Considering the interaction between NSP1 and NSP2, we refer that NSP1 might play a supporting role in the viroplasm-mediated viral replication process.

In summary, we have demonstrated the presence of DpCPV viroplasms and confirmed that NSP2 play the key role for viroplasm formation. This is the first time for observation of viroplasms in insect reoviruses. Furthermore, we found interactions between NSP2 and other viral proteins which helps to elucidate the viroplasms formation and the functions of CPV non-structural proteins in virus replication and assembly mechanisms of CPV.

Acknowledgments

We appreciate the support of the National Key Research and Development Program of China (2017YFD0201206), and the WIV "One-Three-Five" strategic programs (Y602111SA1). We thank the Core Facility and Technical Support of Wuhan Institute of Virology, Chinese Academy of Sciences, for technical assistance with the fluorescence microscopy (Ding Gao), flow cytometry (Juan Min), and electron microscopy (Pei Zhang, Anna Du, and Bichao Xu).

Appendix A. Supplementary data

Supplementary data to this article can be found online at https://doi.org/10.1016/j.virol.2019.05.005.

References

Airenne, K., Hiltunen, M., Turunen, M., Turunen, A., Laitinen, O., Kulomaa, M., Ylä-Herttuala, S.J.G.t., 2000. Baculovirus-mediated periadventitial gene transfer to rabbit carotid artery. Gene Ther. 7, 1499.

Becker, M.M., Peters, T.R., Dermody, T.S., 2003. Reovirus σNS and μNS proteins form cytoplasmic inclusion structures in the absence of viral infection. J. Virol. 77, 5948–5963.

Belloncik, S., 1989. Cytoplasmic polyhedrosis viruses—Reoviridae. Adv. Virus Res. 173–209 Elsevier.

Broering, T.J., Arnold, M.M., Miller, C.L., Hurt, J.A., Joyce, P.L., Nibert, M.L., 2005. Carboxyl-proximal regions of reovirus nonstructural protein muNS necessary and sufficient for forming factory-like inclusions. J. Virol. 79, 6194–6206.

Broering, T.J., Parker, J.S.L., Joyce, P.L., Kim, J., Nibert, M.L., 2002. Mammalian reovirus nonstructural protein μNS forms large inclusions and colocalizes with reovirus microtubule-associated protein μ2 in transfected cells. J. Virol. 76, 8285–8297.

Brookes, S.M., Hyatt, A.D., Eaton, B.T, 1993. Characterization of virus inclusion bodies in bluetongue virus-infected cells. J. Gen. Virol. 74, 525–530.

Chakrabarti, M., Ghorai, S., Mani, S.K., Ghosh, A.K., 2010. Molecular characterization of genome segments 1 and 3 encoding two capsid proteins of Antheraea mylitta cytoplasmic polyhedrosis virus. Virol. J. 7, 181.

Cheng, C., Shao, Y., Su, L., Zhou, Y., Sun, X., 2014. Interactions among Dendrolimus

punctatus cypovirus proteins and identification of the genomic segment encoding its A-spike. J. Gen. Virol. 95, 1532–1538.
Cheng, L., Sun, J., Zhang, K., Mou, Z., Huang, X., Ji, G., Sun, F., Zhang, J., Zhu, P., 2011. Atomic model of a cypovirus built from cryo-EM structure provides insight into the mechanism of mRNA capping. Proc. Natl. Acad. Sci. U. S. A. 108, 1373–1378.
Chiu, E., Coulibaly, F., Metcalf, P., 2012. Insect virus polyhedra, infectious protein crystals that contain virus particles. Curr. Opin. Struct. Biol. 22, 234–240.
Crawford, S.E., Desselberger, U., 2016. Lipid droplets form complexes with viroplasms and are crucial for rotavirus replication. Curr. Opin. Virol. 19, 11–15.
Eaton, B.T., Hyatt, A.D., White, J.R., 1987. Association of bluetongue virus with the cytoskeleton. Virology 157, 107–116.
Echeverry, F., Bergeron, J., Kaupp, W., Guertin, C., Arella, M., 1997. Sequence analysis and expression of the polyhedrin gene of Choristoneura fumiferana cytoplasmic polyhedrosis virus (CfCPV). Gene 198, 399–406.
Fabbretti, E., Afrikanova, I., Vascotto, F., Burrone, O.R., 1999. Two non-structural rotavirus proteins, NSP2 and NSP5, form viroplasm-like structures in vivo. J. Gen. Virol. 80, 333–339.
Fernandez de Castro, I., Zamora, P.F., Ooms, L., Fernandez, J.J., Lai, C.M., Mainou, B.A., Dermody, T.S., Risco, C., 2014. Reovirus forms neo-organelles for progeny particle assembly within reorganized cell membranes. mBio 5.
Goo, T.-W., Yun, E.-Y., Kim, S.-W., Park, K.-H., Hwang, J.-S., Kwon, O.-Y., Kang, S.-W., 2003. Baculovirus expression and biochemical characterization of the Bombyx mori protein disulfide isomerase (bPDI). Int. J. Ind. Entomol. 7, 127–131.
Haatveit, H.M., Nyman, I.B., Markussen, T., Wessel, O., Dahle, M.K., Rimstad, E., 2016. The non-structural protein muNS of piscine orthoreovirus (PRV) forms viral factory-like structures. Vet. Res. 47, 5.
Hagiwara, K., Matsumoto, T, 2000. Nucleotide sequences of genome segments 6 and 7 of Bombyx mori cypovirus 1, encoding the viral structural proteins V4 and V5, respectively. J. Gen. Virol. 81, 1143–1147.
Hagiwara, K., Rao, S., Scott, S.W., Carner, G.R, 2002. Nucleotide sequences of segments 1, 3 and 4 of the genome of Bombyx mori cypovirus 1 encoding putative capsid proteins VP1, VP3 and VP4, respectively. J. Gen. Virol. 83, 1477–1482.
Jia, D., Chen, H., Zheng, A., Chen, Q., Liu, Q., Xie, L., Wu, Z., Wei, T., 2012. Development of an insect vector cell culture and RNA interference system to investigate the functional role of fijivirus replication protein. J. Virol. 86, 5800–5807.
Ke, F., He, L.B., Zhang, Q.Y., 2013. Nonstructural protein NS80 is crucial in recruiting viral components to form aquareoviral factories. PLoS One 8, e63737.
Kunimi, Y., 2007. Current status and prospects on microbial control in Japan. J. Invertebr. Pathol. 95, 181–186.
Li, C., Wen, A., Shen, B., Lu, J., Huang, Y., Chang, Y., 2011. FastCloning: a highly simplified, purification-free, sequence- and ligation-independent PCR cloning method. BMC Biotechnol. 11, 92.
Li, J., Zhou, Y., Lei, C., Fang, W., Sun, X., 2015. Improvement in the UV resistance of baculoviruses by displaying nano-zinc oxide-binding peptides on the surfaces of their occlusion bodies. Appl. Microbiol. Biotechnol. 99, 6841–6853.
Mao, Q., Zheng, S., Han, Q., Chen, H., Ma, Y., Jia, D., Chen, Q., Wei, T., 2013. New model for the genesis and maturation of viroplasms induced by fijiviruses in insect vector cells. J. Virol. 87, 6819–6828.
McNulty, M., Curran, W., McFerran, J.J, 1976. The morphogenesis of a cytopathic bovine rotavirus in Madin-Darby bovine kidney cells. J. Gen. Virol. 33, 503–508.
Mohan, K.V.K., Muller, J., Atreya, C.D., 2003. The N- and C-terminal regions of rotavirus NSP5 are the critical determinants for the formation of viroplasm-like structures independent of NSP2. J. Virol. 77, 12184–12192.
Mori, H., Metcalf, P., 2010. Cypoviruses. In: Asgari, S., Johnson, K.N. (Eds.), Insect Virology. Horizon Scientific Press, pp. 307–323.
Nibert, M.L., Baker, T.S., 2003. CPV, a stable and symmetrical machine for mRNA synthesis. Structure 11, 605–607.
Novoa, R.R., Calderita, G., Arranz, R., Fontana, J., Granzow, H., Risco, C., 2005. Virus factories: associations of cell organelles for viral replication and morphogenesis. Biol. Cell 97, 147–172.
Qin, F., Xu, C., Hu, J., Lei, C., Zheng, Z., Peng, K., Wang, H., Sun, X., 2019. Dissecting the cell entry pathway of baculovirus by single particle tracking and quantitative electron microscopic analysis. J. Virol. 93 e00033-19.
Rao, S., Carner, G., Scott, S., Omura, T., Hagiwara, K.J.A.o.v., 2003. Comparison of the amino acid sequences of RNA-dependent RNA polymerases of cypoviruses in the family Reoviridae. Arch. Virol. 148, 209–219.
Romero-Brey, I., Bartenschlager, R., 2016. Endoplasmic Reticulum: the Favorite Intracellular Niche for Viral Replication and Assembly. Viruses 8.
Roy, P., 2006. Reoviruses: Entry, Assembly and Morphogenesis. Springer Science & Business Media.
Sharpe, A.H., Chen, L.B., Fields, B.N., 1982. The interaction of mammalian reoviruses with the cytoskeleton of monkey kidney CV-1 cells. Virology 120, 399–411.
Shimizu, T., Yoshii, M., Wei, T., Hirochika, H., Omura, T., 2009. Silencing by RNAi of the gene for Pns12, a viroplasm matrix protein ofRice dwarf virus, results in strong resistance of transgenic rice plants to the virus. Plant Biotechnol. J. 7, 24–32.
Tan, Y.R., Sun, J.C., Lu, X.Y., Su, D.M., Zhang, J.Q., 2003. Entry of Bombyx mori cypovirus 1 into midgut cells in vivo. J. Electron. Microsc. 52, 485–489.
Thomas, C., Booth, T., Roy, P., 1990. Synthesis of bluetongue virus-encoded phosphoprotein and formation of inclusion bodies by recombinant baculovirus in insect cells: it binds the single-stranded RNA species. J. Gen. Virol. 71, 2073–2083.
Wei, T., 2006. Pns12 protein of Rice dwarf virus is essential for formation of viroplasms and nucleation of viral-assembly complexes. J. Gen. Virol. 87, 429–438.
Wileman, T., 2007. Aggresomes and pericentriolar sites of virus assembly: cellular defense or viral design? Annu. Rev. Microbiol. 61, 149–167.
Yan, L., Zhang, J., Guo, H., Yan, S., Chen, Q., Zhang, F., Fang, Q., 2015. Aquareovirus NS80 initiates efficient viral replication by retaining Core proteins within replication-associated viral inclusion bodies. PLoS One 10, e0126127.
Yang, J., Cheng, Z., Zhang, S., Xiong, W., Xia, H., Qiu, Y., Wang, Z., Wu, F., Qin, C.-F., Yin, L., 2013. A cypovirus VP5 displays the RNA chaperone-like activity that destabilizes RNA helices and accelerates strand annealing. Nucleic Acids Res. 42, 2538–2554.
Yu, X., Ge, P., Jiang, J., Atanasov, I., Zhou, Z.H., 2011. Atomic model of CPV reveals the mechanism used by this single-shelled virus to economically carry out functions conserved in multishelled reoviruses. Structure 19, 652–661.